

# Inter-subband resistance oscillations in crossed electric and magnetic fields

Scott Dietrich, Sean Byrnes, and Sergey Vitkalov\*

*Physics Department, City College of the City University of New York, New York 10031, USA*

A. V. Goran and A. A. Bykov†

*Institute of Semiconductor Physics, 630090 Novosibirsk, Russia*

(Dated: March 8, 2013)

Quantum oscillations of nonlinear resistance are investigated in response to electric current and magnetic field applied perpendicular to single GaAs quantum wells with two populated subbands. At small magnetic fields current-induced oscillations appear as Landau-Zener transitions between Landau levels inside the lowest subband. Period of these oscillations is proportional to the magnetic field. At high magnetic fields different kind of quantum oscillations emerges with a period, which is independent of the magnetic field. At a fixed current the oscillations are periodic in inverse magnetic field with a period that is independent of the *dc* bias. The proposed model considers these oscillations as a result of spatial variations of the energy separation between two subbands induced by the electric current.

## INTRODUCTION

The magnetotransport phenomena in high-mobility modulation-doped semiconductor structures are commonly studied with only one populated subband ( $E_1$ ), because the electron mobility decreases with filling second subband ( $E_2$ ) due to inter-subband scattering [1]. The latter also gives rise to magneto-inter-subband oscillations (MISO) of the dissipative resistance [2]. In electron systems with two populated subbands MISO have maxima in magnetic fields  $B$  satisfying the relation [3–5]:  $\Delta_{12} = l \cdot \hbar\omega_c$ , where  $\Delta_{12} = E_2 - E_1$  is the energy separation of the bottoms of the subbands,  $\omega_c = eB/m^*$  is cyclotron frequency,  $m^*$  is effective electron mass and  $l$  is a positive integer. In contrast to Shubnikov de Haas (SdH) oscillations the MIS-oscillations exist at high temperature  $kT > \hbar\omega_c$ . An interference of these oscillations with phonon-induced oscillations has been reported [6].

At small quantizing magnetic fields a finite electric current induces several additional nonlinear phenomena. At low temperatures small currents decrease considerably the resistance. The dominant mechanism, inducing the resistance drop, is a peculiar Joule heating (quantal heating), which produces a non-uniform spectral diffusion of electrons over the quantized spectrum. The spectral diffusion is stabilized by inelastic processes ("inelastic" mechanism) [7]. The heating is observed and studied recently [8–11]. At higher currents electron transitions between Landau levels occur due to an elastic electron scattering on impurities in the presence of electric field [12, 13]. The transitions increase the resistance, which was observed in electron systems both with a single occupied subband [14–16] and with multi-subband occupation [17–20]. In the last case an interference of the magneto-inter-subband quantum oscillations (MISO) with the current induced inter-level scattering was reported.

Recent investigations of the nonlinear transport in

stronger magnetic fields reveal another kind of current-induced resistance oscillations in electron systems with a single band occupation [21]. These oscillations occur in electric fields that are significantly smaller than the one required for the current-induced Landau-Zener transitions between Landau levels [12]. The period of the current-induced oscillations is found to be independent of the magnetic field. The oscillations are considered to be a result of spatial variations of the electron filling factor (electron density  $\delta n$ ) with the applied electric field.

In this paper we report an observation of current-induced resistance oscillations of the dissipative resistance in electron systems with two populated subbands. Two kinds of oscillations are detected. At small magnetic fields we observed resistance oscillations with a period proportional to the magnetic field. We found that these oscillations are related to the current induced Landau-Zener transitions between Landau levels [12, 17, 19]. At higher magnetic fields another type of the resistance oscillations emerges with a period that is independent of the magnetic field. In the paper these oscillations are studied at high temperatures at which only MIS-oscillations are present.

Despite a similarity between the current induced oscillations with the  $B$ -independent period, which are found in single subband systems [21] and the oscillations reported in this paper, there is at least one distinct feature to distinguish the two. Namely the oscillations in the two-subband systems occur at high temperatures  $kT \gg \hbar\omega_c$  and, therefore, the total number of the electron states carrying the electric current (inside the energy interval  $kT$ ) does not oscillate with the Fermi energy (in other words with the total electron density  $n$ ). In this regime the SdH oscillations are damped and in single subband systems the current-induced oscillations are absent [21]. Thus even if both kinds of observed oscillations have a common origin, the oscillations reported in this paper are not directly (simply) related to the spatial variations

of the electron density  $\delta n$  induced by the electric current. Another interesting feature is the phase of these oscillations. The oscillations appear to be quasi-periodic with respect to the applied current but with an apparent  $\pi$ -phase shift with respect to the zero bias. Below we present our findings and provide an interpretation of the obtained results.

### EXPERIMENTAL SETUP

Our samples are high-mobility GaAs quantum wells grown by molecular beam epitaxy on semi-insulating (001) GaAs substrates. The width of the GaAs quantum well is 13 nm. Two AlAs/GaAs type-II superlattices grown on both sides of the well served as barriers, providing a high mobility of 2D electrons inside the well at a high electron density [22]. Two samples were studied with electron density  $n_{1,2} = 8.09 \times 10^{15} \text{ m}^{-2}$  and mobility  $\mu_1 = 121 \text{ m}^2/\text{Vs}$  and  $\mu_2 = 73 \text{ m}^2/\text{Vs}$ .

The studied 2D electron systems are etched in the shape of a Hall bar. The width and the length of the measured part of the samples are  $d = 50 \mu\text{m}$  and  $L = 450 \mu\text{m}$ . To measure the resistance we use the four probes method. Direct electric current  $I_{dc}$  ( $dc$  bias) is applied simultaneously with 12 Hz  $ac$  excitation  $I_{ac}$  through the same current contacts ( $x$ -direction). The longitudinal  $ac$  ( $dc$ ) voltage  $V_{xx}^{ac}$  ( $V_{xx}^{dc}$ ) is measured between potential contacts displaced  $450 \mu\text{m}$  along each side of the sample. The Hall voltage  $V_H$  is measured between potential contacts displaced  $50 \mu\text{m}$  across the electric current in  $y$ -direction.

The current contacts are separated from the measured area by a distance of  $500 \mu\text{m}$ , which is much greater than the inelastic relaxation length of the 2D electrons  $L_{in} = (D\tau_{in})^{1/2} \sim 1 - 5 \mu\text{m}$ . The longitudinal and Hall voltages were measured simultaneously, using two lockin amplifiers with  $10 \text{ M}\Omega$  input impedances. The potential contacts provided insignificant contribution to the overall response due to small values of the contact resistance (about  $1 \text{ k}\Omega$ ) and negligibly small electric current flowing through the contacts.

Measurements were taken at different temperatures and magnetic fields in a He-3 insert inside superconducting solenoid. Samples and a calibrated thermometer were mounted on a cold copper finger in vacuum. Magnetic field was applied perpendicular to the 2D electron layers.

### RESULTS

Figure 1 presents the dependence of the dissipative resistance on the magnetic field at temperature  $T = 4.35 \text{ K}$ . At this temperature  $kT > \hbar\omega_c$  and Shubnikov de Haas oscillations are suppressed at  $B < 0.5 \text{ T}$ . The maximums of the observed magneto-intersubband oscillations (MISO) are due to the enhancement of electron elastic scattering,

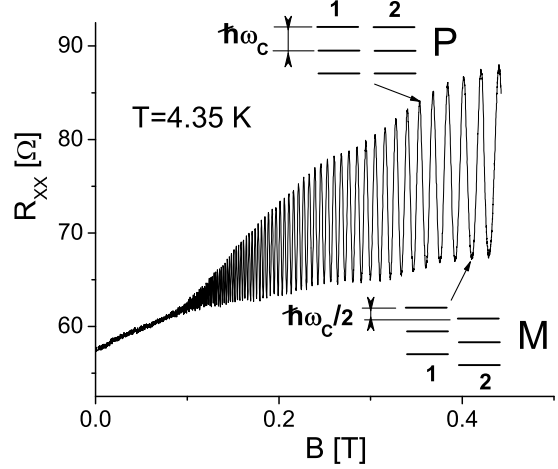


FIG. 1: Dependence of the resistance  $R_{xx}$  on magnetic field with no  $dc$  bias applied. Sample N1.

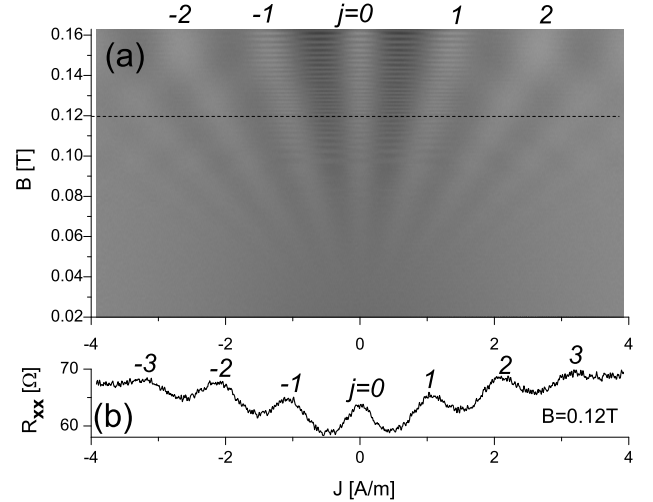


FIG. 2: a) Dependence of differential resistance  $R_{xx}$  on magnetic field and averaged density of electric current  $J$ ; (b) Dependence of the resistance on the current density  $J$  at fixed magnetic field as labeled. Index  $j = \pm 1, \pm 2, \dots$  numerates Landau-Zener transitions inside lowest subband, which obey Eq.(1).  $T = 5.1 \text{ K}$ . Sample N1.

which occurs when the Landau levels in two subbands are lined up with each other (state P in Fig.1). At this condition elastic electron transitions occur between the subbands, increasing the total electron scattering rate and, thus, the resistance. Minima of the oscillations occur when the Landau levels in one subband are between the levels of another subband. In this condition the elastic electron scattering between subbands is suppressed (state M in Fig.1)[5].

Figure 2(a) presents differential resistance  $R_{xx}$  at different averaged density of the electric current  $J =$

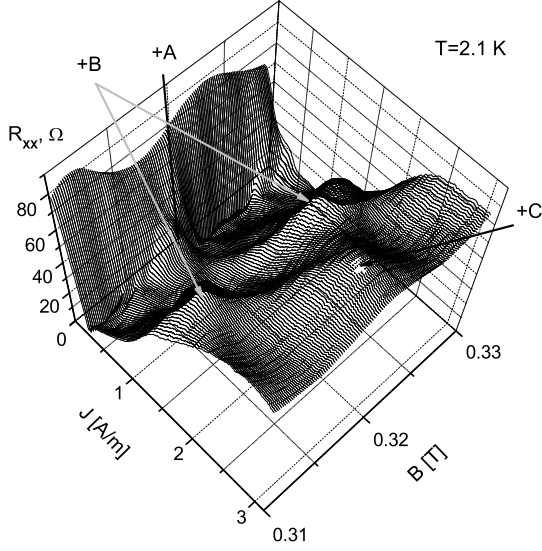


FIG. 3: Dependence of resistance  $R_{xx}$  on magnetic field and current density  $J$ . Labels +A, +B and +C indicate different maxima induced by dc bias.  $T=2.1$  K. Sample N1.

$I_{dc}/(d = 50\mu)$  and small magnetic fields. The differential resistance oscillates with the dc bias. An example of the oscillations is shown in figure 2(b) at fixed magnetic field  $B=0.12$  Tesla. The dependence is a horizontal cut of the 2D plot and is shown by the dashed line in Fig.2(a). Position of a resistance maximum  $j$  is proportional to the magnetic field and satisfies the following relation:

$$2eE_j R_c^{(1)} = j \cdot \hbar\omega_c, \quad (1)$$

where  $E_j$  is the electric field (mostly the Hall electric field in the sample) corresponding to the maximum  $j$ ,  $R_c^{(1)}$  is the cyclotron radius of electrons in the first subband (the lowest subband) and  $j = 0, 1, 2, \dots$  is an integer. Eq.(1) describes Landau-Zener transitions between Landau levels in the first subband[12].

At a higher resolution the data shows oscillations of the magnitude of the maxima  $j = \pm 1$  with the magnetic field at  $B > 0.1$  (T). The oscillations are periodic in inverse magnetic field and are in-phase with the intersubband oscillations at zero dc bias ( $j = 0$ ). Similar oscillations are observed for the minimum between  $j = 0$  and  $j = \pm 1$  maxima. These oscillations are shifted by phase  $\pi$  with respect to the oscillations of the maxima  $j = 0, \pm 1$ . The observed oscillations appear as an interplay between the dc bias induced Landau-Zener transitions between Landau levels inside the lowest subband and the intersubband transitions, which are periodic in inverse magnetic field  $1/B$ . At higher dc biases ( $|j| > 1$ ) the amplitude modulation with the  $1/B$  periodicity disappears. In particular no amplitude modulation is found for  $j = \pm 2, 3$  maxima.

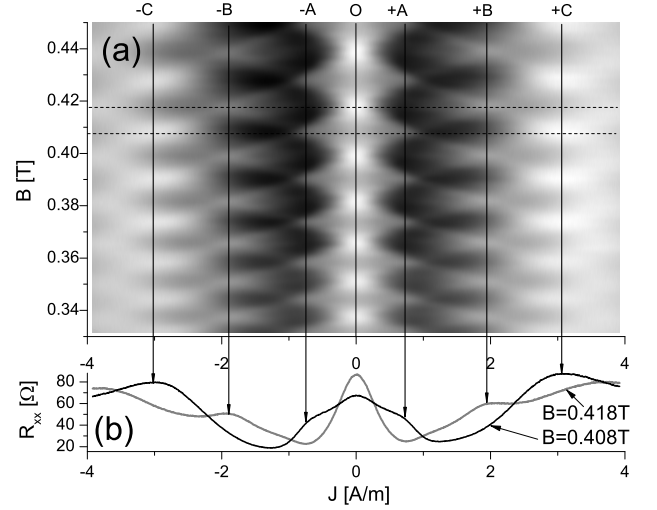


FIG. 4: (a) Dependence of resistance  $R_{xx}$  on magnetic field and current density  $J$ , indicating strong correlation of features  $\pm A$  and  $\pm C$  with MISO minima and features  $\pm B$  with MISO maxima. (b) Dependence of  $R_{xx}$  on current density  $J$  at magnetic field  $B=0.418$  T corresponding to MISO maximum and at magnetic field  $B=0.408$  T corresponding to MISO minimum.  $T=4.7$  K. Sample N1.

Figure 3 presents a typical nonlinear response at a high magnetic field. The response is symmetric with respect to applied dc bias and is shown for the positive bias. There are several distinct features, which appear with the dc bias. The features are labeled in the figure. Firstly we discuss evolution of the resistance with the dc bias at minimum of a MIS oscillation (state  $M$  in fig.1). When the dc bias is applied the resistance falls down and, then, develops a shoulder labeled by symbol +A. The initial drop of the resistance is mostly due to the quantal heating. Further increase of the dc current leads to formation of a maximum labeled by symbol +C.

When the dc bias is applied to state  $P$  (see fig.1), corresponding to maximum of a MIS oscillation, the resistance drops much more abruptly and significantly in comparison with the previous case. At low temperatures the resistance drop reaches zero and forms zero resistance state (ZDRS)[18, 23–25]. Further increase of the dc bias leads to the formation of a maximum labeled by symbol +B.

An evolution of the discussed features with the magnetic field is shown in figure 4(a). The figure demonstrates that the positions of all features ( $\pm A$ ,  $\pm B$ ,  $\pm C$ ) are essentially independent of the magnetic field. Figure 4(b) presents horizontal cuts of the 2D plot through a maximum ( $B=0.418$  T) and a minimum ( $B=0.408$  T) of the inter-subband quantum oscillations.

Figure 5 presents an overall behavior of the quantum oscillations in a broad range of magnetic fields and dc biases. The data was obtained on sample N2. The fig-

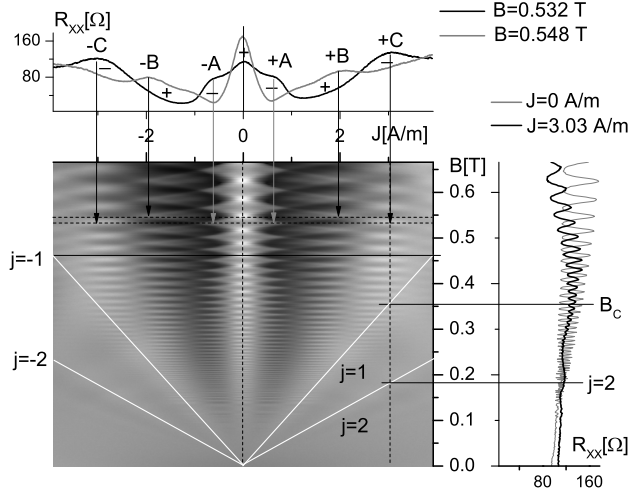


FIG. 5: Evolution of differential resistance with magnetic field and current density in broad range of magnetic fields. White straight lines indicate Landau-Zener transitions which obey Eq.(1). Upper panel presents horizontal cut through MISO maximum at  $B=0.548$  T (gray line) and cut through MISO minimum at  $B=0.532$  T (black line). Sign  $+$ ( $-$ ) indicates regions of current density  $J$ , inside which the current induced oscillations have  $0(180)$  degree phase shift with respect to MIS-oscillations at  $J=0$  A/m. Right panel presents two vertical cuts of the 2D plot taken at current densities as labeled. Magnetic field dependence at  $J=3.03$  A/m indicates strong reduction of the resistance oscillations at  $B < B_c$  inside the region corresponding to Landau-Zener transitions.  $T=5$  K. Sample N2.

ure shows the crossover of the intraband Landau-Zener transitions, obeying Eq.(1), and the oscillations marked as  $\pm A$ ,  $\pm B$ ,  $\pm C$ , which have the MISO periodicity. The apparent crossover occurs near the Landau-Zener transition corresponding to  $j = \pm 1$ . Namely the oscillations with  $1/B$  MISO periodicity occurs at magnetic fields  $B_c$  corresponding to

$$\hbar\omega_c \geq 2eE_1 R_c^{(1)}. \quad (2)$$

At smaller magnetic fields  $B < B_c$  the oscillations are significantly reduced. Two vertical cuts of the 2D plot taken at different currents are shown in the right panel of Fig. 5. The curve taken at  $J=3.03$  A/m shows the strong reduction of the oscillations at  $B < B_c$  in a comparison with the MISO at  $J=0$  A/m. Thus the main intraband Landau-Zener transition ( $j = \pm 1$ ) forms a boundary below which the current induced oscillations with  $1/B$  intersubband periodicity are strongly damped.

The upper panel of Fig. 5 shows two horizontal cuts of the 2D plot. Black solid line presents dependence of the resistance  $R_{xx}$  on  $dc$  bias taken at  $B=0.532$  (T) corresponding to a minimum of MISO. The grey line presents the dependence taken at  $B = 0.548$  (T) corresponding to

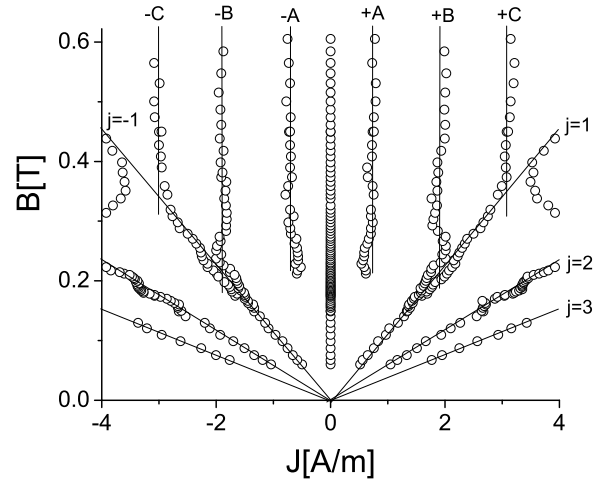


FIG. 6: Positions of resistance maxima and different magnetic fields and current density. Two kind of oscillations are observed: in magnetic fields at and below  $B_c$ , which satisfy Eq.(2), the maxima correspond to Landau-Zener transitions in lowest subband that obey Eq.(1). Solid straight lines at  $j = \pm 1, 2$ , and  $3$  represent the equation. At  $B > B_c$  the resistance maxima follow the vertical solid lines representing features  $\pm A$ ,  $\pm B$  and  $\pm C$  shown on Fig.3,4,5. The crossover between two kind of oscillations occurs at  $B = B_c$  presented by line  $j = \pm 1$ . Sample N1.

a MISO maximum. The two curves intersect at 8 points. These intersections mark the regions at which the oscillations with MISO periodicity changes their phase by  $\pi$ . At the intersections the oscillations are nearly vanished. Sign  $+$  indicates the region between two intersections in which the oscillations are in-phase with the MISO, whereas sign  $-$  indicates the regions in which the oscillations are shifted by phase  $\pi$  with respect to the MISO.

Figure 6 presents an accurate position of the resistance maxima with  $1/B$  periodicity at different currents and magnetic fields for sample N1. The figure indicates clearly that at  $B = B_c$  ( $j = \pm 1$ ) the resistance maxima follow the main Landau-Zener transition  $j = \pm 1$  whereas at  $B > B_c$  the maxima are nearly independent on magnetic field (features  $\pm A$ ,  $\pm B$ ,  $\pm C$ ). The solid lines  $j = \pm 1$  mark the boundary between the two kinds of oscillations. The lines obey eq.(1) at  $j = \pm 1$  with the cyclotron radius  $R_c^1$  corresponding to the lowest subband. The complete theory of the current induced oscillations of the resistance of 2D electron system with two populated subbands is not available in a general case. The case of a bilayer electron system with two closely spaced and almost equally populated electronic subbands has been studied recently[17, 19]. These results are in qualitative agreement with the present data at small magnetic fields  $B < B_c$ .

At high magnetic fields  $B > B_c$  figures 5 and 6 presents new kind of the current induced quantum oscillations. A

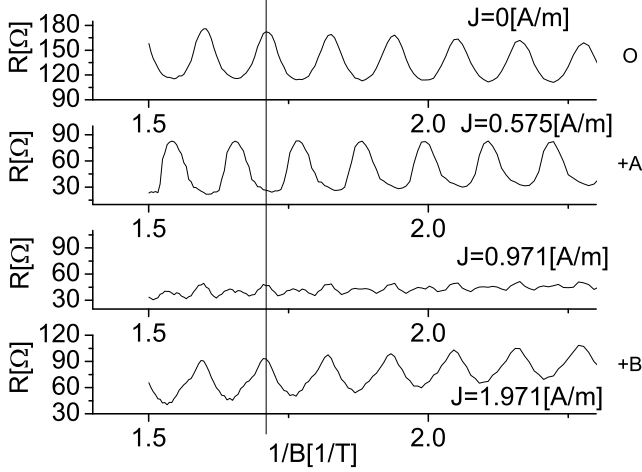


FIG. 7: Dependence of resistance on inverse magnetic field at different dc biases as labeled.  $T=5$  K. Sample N2.

striking feature of these oscillations is the independence of the position of these oscillations on magnetic field. An interesting property of these oscillations is the region in which the oscillations occur. Figures 5, 6 show that these oscillations start at the line corresponding to Landau-Zener transitions at  $j = \pm 1$  in the lowest subband and propagate to higher magnetic fields. Another interesting property is an apparent quasi-periodicity of the oscillations with applied current. Namely the features  $\pm A$ ,  $\pm B$ ,  $\pm C$  are displaced by about the same value of the electric current density from each other:  $\delta J \sim 1.27$  (A/m). The phase of the oscillations is shifted by  $\pi$  with respect to zero dc bias. It seems strange that the MIS-oscillations ( $J=0$  A/m) are not a part of this periodic set.

Figure 7 demonstrates the  $1/B$  periodicity and the phase of the current induced oscillations at different dc biases as labeled. The figure indicates that oscillations at  $J=1.97$  (A/m) (B+ feature) are in phase with MISO, whereas oscillations at  $J=0.575$  A/m (A+ feature) are shifted by  $\pi$  with respect to MISO. Figure 7 shows also the strong reduction of the oscillations at  $J=0.971$  A/m. At this current the oscillations change phase by  $\pi$ . The current corresponds to the intersection of two curves shown in upper panel of Fig.5.

The  $1/B$  periodicity of the oscillations and the magnetic field independence of the electric current  $I_{dc}$ , inducing the oscillations at  $B > B_c$ , indicates a similarity of these quantum oscillations with the current induced quantum oscillations reported recently in Ref.[21]. Below we consider a model, which is, in many respects, analogous to one described in Ref.[21]. The model reproduces the main properties of the observed quantum oscillations.

## MODEL AND DISCUSSION

Current induced quantum oscillations with  $1/B$  periodicity were recently observed in 2D electron systems with a single occupied subband [21]. The oscillations occur in a strong magnetic field at which Shubnikov de Haas oscillations (SdH)[26] are well developed. With respect to the electric current the oscillations are periodic with a period that is independent on the magnetic field. The proposed model considers the oscillations as result of a variation of the electron filling factor with the dc bias. In contrast to SdH oscillations, the variation appears across the sample and is related to a spatial change of the electron density  $\delta n$ . If the change  $\delta n$  is comparable with the number of electron states in a Landau level  $n_0 = m/(\pi\hbar^2) \cdot \hbar\omega_c$ , then one should expect a variation of the electron resistivity. The spatial variation of the resistivity leads to oscillations of the sample resistance[21].

MIS-oscillations occur due to a periodic enhancement of the inter-subband scattering, when Landau levels in two subbands are line up as shown in Fig.1. MISO have maxima in magnetic fields  $B$  satisfying the relation [3–5]:  $\Delta_{12} = i\hbar\omega_c$ , where  $\Delta_{12} = E_2 - E_1$  is the energy separation of the bottoms of the subbands and  $i$  is an integer. In contrast to SdH oscillations the MIS-oscillations exist at high temperature  $kT > \hbar\omega_c$  and are insensitive to variations of the Fermi energy and/or electron density  $n$  for non-interacting 2D carriers.

For interacting electron systems the situation is different. Recent direct experiment indicates that gap  $E_0$  between conducting and valence bands of 2D electron systems formed in GaAs quantum wells depends considerably on the electron density  $n$  [27]. This observation opens a way to consider the dependence of the energy separation between two subbands  $\Delta_{12}$  on the electron density as a mechanism leading to the current induced quantum oscillations in magnetic fields  $B > B_c$ . Indeed the experiment Ref.[27] demonstrated about one percent change of the gap  $E_0$  at a Hall voltage  $V_H=75$  (mV) in magnetic field  $B=0.3$  (T). The Hall voltage is comparable with the one observed in our experiment:  $V_H \approx 50$  mV at  $B=0.35$  (T) and  $J=4$  (A/m). At  $B=0.35$  (T) the phase of the MISO  $2\pi\Delta_{12}/\hbar\omega_c \approx 2\pi \cdot 30$  requires about 3 percent change of the inter-subband energy separation  $\Delta_{12}$  to make an additional MIS-oscillation cycle. The comparison indicates a feasibility of the proposed mechanism, taking into account that in our samples the GaAs quantum well is sandwiched between conducting layers, which enhance significantly the electron screening and, therefore, the variations of the electron density  $\delta n$  with the dc bias [21].

In the model described below we assume that the dc bias-induced variation of the electron density  $\delta n(r)$  changes the energy separation  $\Delta_{12}(n)$  between two subbands across samples. Since relative variations of the

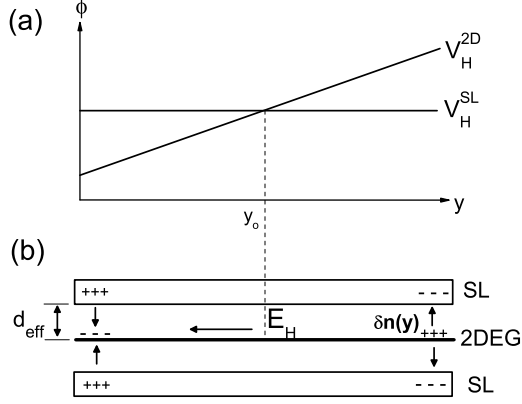


FIG. 8: Dependence of the electric potential on position  $y$  in the direction perpendicular to the electric current in strong magnetic field. Line  $V_H^{2D}$  describes the potential in GaAs quantum well, in which strong Hall effect is developed. Line  $V_H^{SL}$  describes the potential in the highly resistive superlattice layer, in which the Hall voltage is negligibly small due to the negligibly small current in the layer.

electron density is small  $\delta n/n \ll 1$ , we will consider only the linear term of the dependence  $\Delta_{12}(n)$ :

$$\Delta_{12}(n) = \Delta_0 + \gamma \delta n(r), \quad (3)$$

where  $\Delta_0$  is the energy separation at zero dc bias and the parameter  $\gamma$  is a constant. The following consideration is qualitatively similar to the model described in detail in Ref.[21]. Below we describe the main parts of the model omitting some details.

The conducting 2D electron system in the GaAs quantum well is sandwiched between two layers of AlAs/GaAs superlattices (SL) of the second kind [22]. The parameters of the superlattices are adjusted to set the system close to a metal-insulator transition. At this condition the barely-conducting SL layers efficiently screen electric charges but do not contribute considerably to the overall conductivity of the structure. Electric contacts connect the GaAs and the SL layers. Thus the system is considered as a set of parallel conductors. At zero magnetic field the distribution of the electric potential driving the current is the same in all layers due to the same shape of the conductors. That is to say at  $B=0$  the potential difference between different layers is absent. In the poorly conducting SL layers the electric current is several order of magnitude smaller than the one in the highly conducting GaAs quantum well.

The layers have a different distribution of the electric potential in a strong magnetic field, at which  $\omega_c \tau_{tr}^{2D} \gg 1$  and  $\omega_c \tau_{tr}^{SL} \ll 1$ , where  $\tau_{tr}^{2D}$  and  $\tau_{tr}^{SL}$  are transport times in the GaAs and in the SL layers. At  $\omega \tau_{tr}^{2D} \gg 1$  the elec-

tric field in the GaAs layer is almost perpendicular to the current due to the strong Hall effect. In contrast the very small electric current in the SL layer induces a Hall voltage, which is negligible. The Hall voltages are shown in Fig.8 (a) for small currents ( linear response). Figure 8(b) presents distribution of electric charges in the structure. Electric charges are accumulated near the edges of the 2D highly conducting GaAs layer, inducing the Hall electric field  $E_H$ . The charges are partially screened by charges accumulated in the conducting SL layers.

Due to the small Hall voltage  $E_H^{SL}$  and the absence of the electric current across the system the change of the electric potential  $\phi^{SL}(y)$  in the SL layer is negligibly small. Below we consider the potential  $\phi^{SL}$  as a constant. Due to a finite screening length  $\lambda_s$  in the SL layer the charge accumulation occurs at a distance  $d \sim \lambda_s$ . Below we approximate the charge distribution by a charged capacitor with an effective distance  $d_{eff}$  between conducting plates.

The proposed model considers a long 2D Hall bar with a width  $L_y$ [28, 29]. Electric current is in  $x$ -direction and the Hall electric field is in  $y$ -direction. In a long conductor the electric field  $\vec{E} = (E_x, E_y)$  is independent on  $x$ , due to the uniformity of the system in  $x$  direction:

$$\frac{\partial E_x}{\partial x} = \frac{\partial E_y}{\partial x} = 0 \quad (4)$$

For a steady current Maxwell equations yield:

$$\frac{\partial E_x}{\partial y} = \frac{\partial E_y}{\partial x} \quad (5)$$

Eq.(4) and eq.(5) indicate, that the  $x$  component of the electric field is the same at any location:  $E_x = E = \text{const.}$

Boundary conditions and the continuity equation require that the density of the electric current in  $y$  direction is zero:  $J_y = 0$  and therefore,

$$E_x = \rho_{xx} J_x \quad E_y = \rho_{yx} J_x \quad (6)$$

where  $\rho_{xx}$  and  $\rho_{yx}$  are longitudinal and Hall components of the resistivity tensor [30]. We approximate the MIS-oscillations of the resistivity by a simple expression [5]:

$$\rho_{xx}(n(y)) = \rho_D [1 + \alpha \cdot \cos(\frac{2\pi \Delta_{12}}{\hbar \omega_c})] \quad (7)$$

where  $\rho_D$  is Drude resistivity, and  $\alpha$  describes the amplitude of the quantum oscillations.

An electrostatic evaluation of the voltage between conducting layers, shown in Fig.8(b), yields:

$$\phi^{2D}(y) = \phi^{SL} + \frac{e \delta n(y) d_{eff}}{2 \epsilon \epsilon_0} \quad (8)$$

where  $\phi^{2D}$  and  $\phi^{SL}$  are electric potentials of the GaAs (2DEG) and superlattice (SL) layers, and  $\epsilon$  is permittivity of the SL layer. Expressing the electron density  $\delta n$  in terms of electric potential  $\phi^{2D}$  from Eq.(8) and substituting the relation into eq.(3) and then into eq.(7) one can find dependence of the resistivity on the electric potential:  $\rho_{xx}(\phi^{2D})$ .

The relation  $E_y = -d\phi^{2D}/dy$  together with eq.(6) yields:

$$-\frac{d\phi^{2D}}{dy}\rho_{xx}(\phi^{2D}) = \rho_{yx}E \quad (9)$$

Separation of the variables  $\phi^{2D}$  and  $y$  and subsequent integration of eq.9 between two sides of the 2D conductor ( $y$ -direction) with corresponding electric potentials  $\phi_1$  and  $\phi_2$  yield the following result:

$$\begin{aligned} \rho_D(\phi_2 - \phi_1 + \frac{2\alpha}{\beta}[\sin[\frac{\beta}{2}(\phi_2 - \phi_1)] \\ \times \cos[\frac{\beta}{2}(\phi_2 + \phi_1) + \theta_0]]) = \rho_{xy}EL_y \end{aligned} \quad (10)$$

$$\begin{aligned} \beta &= 4\pi\epsilon_0\epsilon\gamma/(ed_{eff}n_0), \\ \theta_0 &= 2\pi\Delta_0/\hbar\omega_c - \beta\phi^{SL}, \end{aligned}$$

where  $L_y$  is a width of the sample. Taking into account that longitudinal voltage is  $V_{xx} = EL_x$ , where  $L_x$  is a distance between the potential contacts, and the Hall voltage  $V_H = \phi_2 - \phi_1 = -\int E_y dy = -\rho_{yx}I$  (see eq.6), the following relation is obtained:

$$V_{xx} = R_D(I - \frac{2\alpha}{\beta\rho_{xy}}[\sin(\frac{\beta\rho_{xy}I}{2}) \cdot \cos[\frac{\beta}{2}(\phi_2 + \phi_1) + \theta_0]]) \quad (11)$$

, where  $R_D = L_x\rho_D/L_y$  is Drude resistance.

Eq.11 is simplified further for two cases corresponding to a minimum and a maximum of MIS-oscillations. In these cases the voltage  $\phi^{2D}(\delta y) - \phi^{SL}$  is expected to be an asymmetric function of the relative position  $\delta y = y - y_0$  with respect to the center of the sample  $y_0$  (as shown in fig. 8) and, thus,  $\phi_1 - \phi^{SL} = -(\phi_2 - \phi^{SL})$  and the argument of the cosine in eq.11 becomes to be independent on the electric current. In these cases the differential resistance  $r_{xx} = dV_{xx}/dI$  is found to be

$$r_{xx} = R_D[1 + \alpha \cdot \cos(2\pi\frac{I}{I_0}) \cdot \cos(\frac{2\pi\Delta_0}{\hbar\omega_c})], \quad (12)$$

where  $I_0 = e^3\hbar d_{eff}n/\epsilon\epsilon_0 m\gamma$ .

Eq. 12 demonstrates oscillations of the differential resistance with the electric current. The period of the oscillations  $I_0$  does not depend on the magnetic field in accordance with the experiment. The amplitude of the MIS-oscillations is strongly modulated by the dc bias. In particular at  $I = I_0/4$  the amplitude is zero. At this node the  $1/B$  periodic oscillations change phase by  $\pi$ . The strong amplitude modulation with the dc bias and the  $\pi$  phase shift at a node agree with the experiment.

Following from Eq.(12) positions of the nodes and anti-nodes of the oscillations with respect to the current  $I_{dc}$  do not agree with the experiment. In accordance with Eq.(12) the nodes occurs at

$$\begin{aligned} J_k &= \frac{I_0}{4} \cdot k, \\ k &= 2i - 1; i = 1, 2, 3, \dots, \end{aligned} \quad (13)$$

where  $k$  is a node index. Upper panel of Fig.5 shows nodes at 0.22, 0.93, 2.41 and 3.91 A/m. Thus the relative positions of the nodes observed in the experiment do not follow the node positions (or index  $k$ ) in Eq.(13). Below we show that the disagreement is reduced significantly taking into account the Joule's heating.

The discussed above model does not take into account the dc heating of the 2D electrons. The Joule heating in systems with a discrete spectrum (quantal heating) has a peculiar form providing strong impact on the electron transport [9]. In electron systems with two subbands occupied the quantal heating inverts the MIS-oscillations [10, 11]. A quantitative account of the heating will not be done in this paper. Instead we will use an analytical approximation of the heating which is valid for two subbands with equal electron population. As shown below the approach yields the positions of the nodes which agree with the experiment.

The expression for the resistivity of 2D electron systems with two equally populated subbands in crossed electric and quantizing magnetic field reads [11]

$$\begin{aligned} \rho_{xx} &= \rho_D[1 + \exp(-\frac{2\pi}{\omega_c\tau_q})\frac{1-3Q}{1+Q}(1 + \cos(\frac{2\pi\Delta_{12}}{\hbar\omega_c}))] \\ Q &= \frac{2\pi^3J^2}{e^2n\omega_c^2} \cdot \frac{\tau_{in}}{\tau_{tr}}, \end{aligned} \quad (14)$$

where  $\tau_q$  is quantum scattering time,  $\tau_{in}$  and  $\tau_{tr}$  are inelastic and transport scattering times. To account the heating we replace Eq.(7) by Eq.(14) and evaluate differential Eq.(9) numerically with fitting parameters approximating the experimental data. Due to a quite rough approximation of the heating, the fitting parameters may deviate significantly from actual physical values. To find the fitting parameter corresponding to the inelastic scattering time we use that the second term of Eq.(14) is zero at  $Q=1/3$  [11]. Assuming that at a small dc bias and low temperatures the quantal heating dominates [9, 11], we related the first node shown in Fig.5 at  $J=0.22$  A/m to the condition  $Q=1/3$ . This yields  $\tau_{in} = 1.8$  ns at  $B=0.53$ T. Using this value we solved Eq.(9) numerically. The result is shown in Fig.9 (a). At small dc bias  $J \approx 0.17$  A/m the figure demonstrates the oscillation node, induced by the heating with a small contribution from the variation of the band separation  $\Delta_{12}$ . Other nodes occur at considerably higher dc biases and are shifted with respect to the nodes shown in Fig.9(b)), which obtained by the numerical evaluation, ignoring the quantal heating ( $Q=0$ ).

At  $Q > 1/3$  the heating not only shift the nodes but also inverts of the oscillations induced by variations of

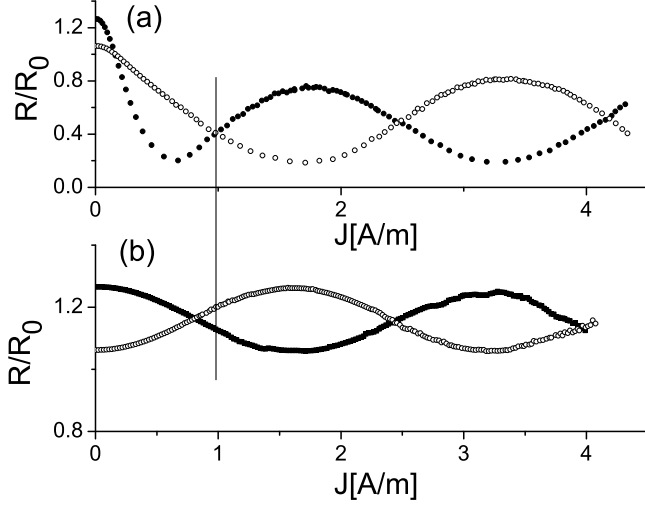


FIG. 9: (a) Numerical simulation of the dependence of differential resistance on dc bias at  $B=0.53$  T. Fitting parameters used in the numerical simulation:  $\tau_{in}=1.8$  ns,  $\tau_q=2.5$  ps and  $\tau_{tr}=45$  ps; electron density  $n=8.09 \cdot 10^{15}$   $1/m^2$ ; effective screening length  $d_{eff}=30$  nm; parameter  $\gamma=1 \cdot 10^{-37}$   $Jm^2$  (see Eq.(3)). (b) Numerical simulation of the dependence of differential resistance on dc bias with the same fitting parameters as in (a) but without dc heating:  $\tau_{in}=0$  ns ( $Q=0$ ). Filled (open) circles present evolution of a MISO maximum (minimum) with the dc bias

the band separation. Namely shown in Fig.9(a) the maximum at  $J=1.75$  A/m is a result of the dc bias induced evolution of the MISO maximum at  $J=0$  A/m. Without the heating the MISO maximum evolves into a minimum at  $J=1.65$  A/m shown in Fig.9(b). Thus the heating inverts minimums to maximums and visa versa. The inversion is directly related to the sign change of the second term in Eq.(14) at  $Q=1/3$ .

The heating and the variation of the band separation affect differently the maximums and minimums of MIS-oscillations. Conversely, quantal heating decreases the resistance at any magnetic field. A variation of the resistance, induced by the change of the band separation, depends on the magnetic field. At a maximum (state P in Fig.(1)), a variation of  $\Delta_{12}$  destroys the level alignment decreasing the inter-band scattering and, thus, the resistance. At a minimum (state M in Fig.(1)), a variation of  $\Delta_{12}$  improves the level alignment and increases the inter-band scattering and the resistance. Thus at a MISO maximum both the heating and the variations of the band separation decreases the resistance whereas at a MISO minimum two mechanisms work against each other. In result the drop of the resistance at a MISO maximum is considerably stronger the one at a MISO minimum. In fact the shoulder (feature +A in Fig.3) is a result of the competition between two mechanisms at a MISO minimum whereas ZDRS states, developed from

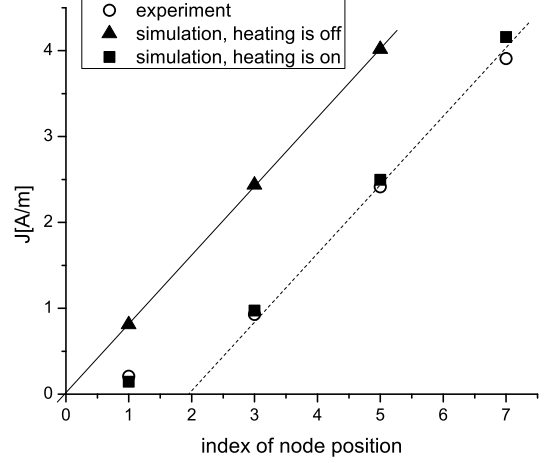


FIG. 10: Position of nodes of dc bias induced oscillations shown in Fig.9 and Fig.5 at different node index  $k$ . Filled triangles present nodes, which are obtained numerically without heating and obey Eq.(13) (solid line). Account of the heating (filled squares) improves significantly agreement with the experiment (open circles). Dashed line is a shift of the solid line to the right by two units (see text for detail).

MISO maximums, is a strong indication of the joint decrease of the resistance due to both mechanisms. The behavior is reproduced in the proposed model. Indeed Fig.9(a) shows that the initial drop of the MISO maximum is considerably stronger than the decrease of the MISO minimum with the dc bias.

Figure 10 presents a comparison of the positions of oscillation nodes, obtained in the model, with the experiment. For the purpose of a comparison, the node positions are plotted versus the index  $k$ , which is defined in Eq.(13). Without the heating nodes of oscillations obey Eq.13. Filled triangles demonstrate this behavior. When the heating is on (filled squares) the first node ( $k=1$ ) is due mostly to the heating. The following nodes ( $k=3, 5$ , and  $7$ ) are due mostly to the variation of the band separation. As shown in the figure the positions of the nodes correlate well with the experimental values (open circles) taken from the upper panel of Fig.5.

The quantal heating produces an additional node of the dc bias induced oscillations. It changes the systematic placement of the node positions described by Eq.(13). In the case of a strong quantal heating (as in Fig.9) the additional node occurs at the very beginning of the resistance evolution. Expected from Eq.(13) node counting can be largely restored by a reduction of the node index by two, which is the difference between consecutive indexes  $k$  in Eq.(13). The corresponding transformation is shown in Fig.10: the dashed line is the shift by two units to the right of the solid line representing index  $k$  in Eq.(13).



## CONCLUSION

Quantum oscillations of nonlinear resistance, which occur in response to electric current and magnetic field applied perpendicular to GaAs quantum wells with two populated subbands, are investigated. At small magnetic fields the current-induced oscillations are found to be related to Landau-Zener transitions between Landau levels inside the lowest subband. The period of these oscillations is proportional to the magnetic field. At high magnetic fields a different kind of quantum oscillations are observed. With respect to the dc bias these resistance oscillations are quasi-periodic with a period that is independent of the magnetic field. At a fixed electric current the oscillations are periodic in inverse magnetic field. The period is independent of the *dc* bias. The proposed model considers these oscillations as a result of joint effect of the Joule heating in the systems with discrete spectrum and the spatial variations of the energy separation between two subbands, which is induced by the electric current. Obtained results indicate the feasibility of considerable modification of the electron spectrum by applied electric current in two dimensional electron systems.

S. V. thanks I. L. Aleiner for valuable help with the theoretical model and discussion. Work was supported by National Science Foundation (DMR 1104503) and the Russian Foundation for Basic Research, project no. 11-02-00925.

---

\* Corresponding author: vitkalov@sci.ccny.cuny.edu

† Novosibirsk State Technical University, 630092 Novosibirsk, Russia

- [1] H. L. Stormer, A. C. Gossard, and W. Weigmann, *Solid State Commun.* **41**, 707 (1982).
- [2] D. R. Leadley, R. Fletcher, R. J. Nicholas et al., *Phys. Rev. B* **46**, 12439 (1992).
- [3] L. I. Magarill and A. A. Romanov, *Sov. Phys. Solid State* **13**, 828 (1971).
- [4] V. M. Polyanovskii, *Sov. Phys. Semicond.* **22**, 1408 (1988).
- [5] M. E. Raikh, T. V. Shahbazyan, *Phys. Rev. B* **49**, 5531 (1994).
- [6] A. A. Bykov, A. V. Goran, and S. A. Vitkalov, *Phys. Rev. B* **81**, 155322 (2010).
- [7] I. A. Dmitriev, M.G. Vavilov, I. L. Aleiner, A. D. Mirlin, and D. G. Polyakov, *Phys. Rev. B* **71**, 115316 (2005).
- [8] Jing-qiao Zhang, Sergey Vitkalov, A. A. Bykov, A. K. Kalagin, and A. K. Bakarov *Phys. Rev. B* **75**, 081305(R) (2007).
- [9] Jing Qiao Zhang, Sergey Vitkalov, and A. A. Bykov *Phys. Rev. B* **80**, 045310 (2009).
- [10] A. A. Bykov, *JETP Lett.* **88**, 64 (2008).
- [11] N. C. Mamani, G. M. Gusev, O. E. Raichev, T. E. Lamas, and A. K. Bakarov, *Phys. Rev. B* **80**, 075308 (2009).
- [12] C. L. Yang, J. Zhang, and R. R. Du, J. A. Simmons and J. L. Reno, *Phys. Rev. Lett.* **89**, 076801 (2002).
- [13] M.G. Vavilov, I.L. Aleiner, and L.I. Glazman, *Phys. Rev. B* **76**, 115331 (2007).
- [14] A. A. Bykov, Jing-qiao Zhang, Sergey Vitkalov, A. K. Kalagin, and A. K. Bakarov, *Phys. Rev. B* **72**, 245307 (2005).
- [15] W. Zhang, H.-S. Chiang, M. A. Zudov, L.N. Pfeiffer, and K.W. West, *Phys. Rev. B* **75**, 041304(R) (2007).
- [16] Yanhua Dai, Z. Q. Yuan, C. L. Yang, R. R. Du, M. J. Manfra, L. N. Pfeiffer, and K. W. West, *Phys. Rev. B* **80**, 041310 (2009).
- [17] A. A. Bykov, *JETP Lett.* **88**, 394 (2008).
- [18] A. A. Bykov, E. G. Mozulev, and S. A. Vitkalov, *JETP Lett.* **92**, 475 (2010).
- [19] S. Wiedmann, G. M. Gusev, O. E. Raichev, A. K. Bakarov, and J. C. Portal, *Phys. Rev. B* **84**, 165303 (2011).
- [20] A. V. Goran, A. K. Kalagin, and A. A. Bykov, *JETP Lett.* **94**, 535 (2011).
- [21] Scott Dietrich, Sean Byrnes, Sergey Vitkalov, D. V. Dmitriev and A. A. Bykov *Phys. Rev. B* **85**, 155307 (2012).
- [22] K. J. Friedland, R. Hey, H. Kostial, R. Klann, and K. Ploog, *Phys. Rev. Lett.* **77**, 4616 (1996).
- [23] A. A. Bykov, J.Q. Zhang, S. Vitkalov, A. K. Kalagin, and A. K. Bakarov, *Phys. Rev. Lett.* **99**, 116801 (2007).
- [24] A. T. Hatke, H.-S. Chiang, M. A. Zudov, L. N. Pfeiffer, and K. W. West, *Phys. Rev. B* **82**, 041304(R) (2010).
- [25] G. M. Gusev, S. Wiedmann, O. E. Raichev, A. K. Bakarov, and J. C. Portal, *Phys. Rev. B* **83**, 041306(R) (2011).
- [26] D. Shoenberg *Magnetic oscillations in metals*, (Cambridge University Press, 1984).
- [27] I. Baskin, B. M. Ashkinadze, E. Cohen, V. V. Belkov, L. N. Pfeiffer, and V. Umansky, *Phys. Rev. B* **84**, 245320 (2011).
- [28] A. A. Shashkin, V. T. Dolgoplov, and S. I. Dorozhkin, *Sov. Phys. JETP* **64**, 1124 (1986).
- [29] M. I. Dyakonov, *Solid State Comm.* **78**, 817 (1991).
- [30] J. M. Ziman *Principles of the theory of solids*, (Cambridge at the University Press, 1972).
- [31] T. Ando, A. B. Fowler, and F. Stern, *Rev. of Mod. Phys.* **54**, 437 (1982).